

# Scattered light corrections to Sun photometry: analytical results for single and multiple scattering regimes

Alexander A. Kokhanovsky

*Institute of Remote Sensing, O. Hahn Allee 1, D-28334 Bremen, Germany*

Received July 3, 2006; revised September 27, 2006; accepted November 3, 2006;  
posted November 10, 2006 (Doc. ID 72588); published March 14, 2007

Analytical equations for the diffused scattered light correction factor of Sun photometers are derived and analyzed. It is shown that corrections are weakly dependent on the atmospheric optical thickness. They are influenced mostly by the size of aerosol particles encountered by sunlight on its way to a Sun photometer. In addition, the accuracy of the small-angle approximation used in the work is studied with numerical calculations based on the exact radiative transfer equation. © 2007 Optical Society of America

OCIS codes: 010.0010, 010.1110, 010.1320.

## 1. INTRODUCTION

Atmospheric optical thickness  $\tau$  is a crucial parameter that influences climate and weather. For clear skies, this parameter is also a good indicator of atmospheric pollution. The value of  $\tau$  for cloudless cases is determined by molecular and aerosol scattering and absorption. The molecular contribution is rather robust and can be subtracted from the registered signal to yield the aerosol optical thickness  $\tau_a$ , which is an important parameter for a number of applications.

On one hand, the measurements of  $\tau$  are quite straightforward. One must direct a photometer at the Sun and use the exponential attenuation law to determine the atmospheric optical thickness. However, many complications arise, which often prevent the correct determination of  $\tau$ . This includes the problem of the calibration (e.g., for different temperature regimes) and also the correction with respect to the scattered light.<sup>1</sup> A Sun photometer has a finite field of view (FOV). Therefore, the scattered light enters the instrument, increasing the registered signal. This leads to the underestimation of the derived optical thickness if the results of measurements are not processed correctly. This issue has been studied by many authors.<sup>2–6</sup>

The task of this work is to propose analytical equations that can be used for the estimation of corresponding correction factors both in single and multiple scattering regimes, depending on the size of particles and also on the atmospheric optical thickness.

## 2. SINGLE SCATTERING APPROXIMATION

The power as received by a ground photometer looking in the direction of the Sun can be expressed as<sup>7</sup>

$$F = \int_{\Omega_0} A I d\Omega, \quad (1)$$

where  $A$  is the receiving cross section,  $d\Omega = \sin \vartheta d\vartheta d\phi$  is the elementary solid angle,  $\vartheta$  is the zenith angle,  $\phi$  is the

azimuth, and  $I$  is the light intensity in the FOV of the instrument defined by the solid angle  $\Omega_0$ . It follows from Eq. (1) that

$$F = \Sigma \int_{\Omega_0} I d\Omega, \quad (2)$$

where the area  $\Sigma$  is a characteristic of a given instrument. The intensity as received by a photometer can be represented as a sum of the direct light component  $I_{dir}$  and the diffused intensity  $I_{dif}$ . One can easily derive the following expression for the direct light intensity<sup>7</sup>:

$$I_{dir} = E_0 \exp(-x) \delta(\Omega_0 - \Omega), \quad (3)$$

where  $\delta(\Omega_0 - \Omega)$  is the delta function,  $x = \tau/\mu_0$ ,  $\mu_0$  is the cosine of the incidence angle,  $\tau$  is the optical depth along the local vertical, and  $E_0$  is the top-of-atmosphere solar irradiance. It follows for the diffused light component in the framework of the single scattering approximation—assuming that the zenith observation and incidence angles coincide<sup>7</sup>—

$$I_{dif} = \frac{\omega_0 E_0 p(\theta) x \exp(-x)}{4\pi}, \quad (4)$$

where  $\omega_0 = K_{sca}/K_{ext}$  is the single scattering albedo,  $K_{sca}$  is the scattering coefficient,  $K_{ext}$  is the extinction coefficient,  $p(\theta)$  is the phase function, and  $\theta$  is the scattering angle. We obtain from Eqs. (2)–(4) that

$$F = \Sigma E_0 \exp(-x) (1 + f x), \quad (5)$$

where

$$f = \frac{\omega_0}{2} \int_0^{\theta_0} p(\theta) \sin \theta d\theta, \quad (6)$$

and  $\theta_0$  is the half-FOV angle. Taking into account that  $f x \rightarrow 0$  for singly scattering media, we have approximately from Eq. (5)

$$F = \Sigma E_0 \exp[-(1-f)x]; \quad (7)$$

therefore,  $x = (1-f)^{-1}x_0$ , where  $x_0 = \ln(\Sigma E_0/F) \equiv \tau_0/\mu_0$ , and  $\tau_0$  is the so-called apparent optical thickness. Also we can write

$$\tau = C\tau_0, \quad (8)$$

where

$$C = \frac{1}{1-f} \quad (9)$$

is the correction factor (CF). Equations (8) and (9) were derived by Shiobara and Asano<sup>2</sup> in a way similar to that shown above and used for studies of diffuse light corrections to Sun photometry and pyrheliometry.<sup>6</sup>

Clearly, it follows that  $f=0$  at  $\theta_0=0$  [see Eq. (6)] and  $\tau = \tau_0$  then. In reality,  $\theta_0 \neq 0$ ,  $0 < f < 1$ , and the true value of  $\tau$  is larger than the apparent optical thickness  $\tau_0$ .  $C$  takes values between approximately 1 and 2 for most practical cases, depending on the size of particles and the actual value of the FOV angle.<sup>6</sup> Even larger values of  $C$  are possible if  $\theta_0$  is not small.

Let us estimate  $f$  for large spherical particles of radius  $r$  much larger than the wavelength  $\lambda$ . Because  $\theta_0 \rightarrow 0$  for modern spectrophotometers, we can use the following approximation<sup>8</sup> for the normalized Mie intensity  $i(\theta)$  in the small-angle scattering region ( $\theta \rightarrow 0$ ) for a spherical particle of radius  $r$  and arbitrary complex refractive index  $m$ :

$$i(\theta) = \frac{\rho^4}{4} \Phi^2(\theta\rho), \quad (10)$$

where  $\rho = kr$ ,  $k = 2\pi/\lambda$ , and

$$\Phi(\theta\rho) = \frac{2J_1(\theta\rho)}{\theta\rho}, \quad (11)$$

where  $J_1(\theta\rho)$  is the Bessel function. Equation (10) has a high accuracy<sup>8</sup> as  $\theta \rightarrow 0$ ,  $\rho \rightarrow \infty$ , and  $p \equiv 2|m-1|\rho \rightarrow \infty$ .

The phase function of the spherical polydispersion is defined as<sup>9</sup>

$$p(\theta) = \frac{2\pi N \int_0^\infty \varphi(r)(i_1 + i_2)dr}{k^2 K_{sca}}, \quad (12)$$

where  $\varphi(r)$  is the particle size distribution (PSD) and

$$K_{sca} = N \int_0^\infty \pi r^2 \varphi(r) Q_{sca} dr. \quad (13)$$

Here  $Q_{sca}$  is the scattering efficiency factor determined from the Mie theory. The simple analytical expression for the scaled phase function  $\hat{p}(\theta) = \omega_0 p(\theta)$  can be derived at small angles  $\theta$  using Eqs. (10)–(12) and also the fact that  $i_1 \approx i_2 \approx i$  at small angles. So it follows that

$$\hat{p}(\theta) = \frac{2\langle J_1^2(k\theta r) \rangle}{\theta^2}, \quad (14)$$

where we used the fact that  $K_{ext} = 2\pi N M_2$  ( $M_2$  is the second moment of PSD) for large particles<sup>8</sup> and angular brackets mean

$$\langle y(k\theta r) \rangle = \frac{\int_0^\infty y(k\theta r) r^2 \varphi(r) dr}{\int_0^\infty r^2 \varphi(r) dr} \quad (15)$$

for arbitrary function  $y(k\theta r)$ . One obtains from Eq. (14) at  $\theta=0$  that

$$\hat{p}(0) = \frac{k^2 M_{42}}{2}, \quad (16)$$

where  $M_{42} \equiv M_4/M_2$ , and

$$M_n = \int_0^\infty r^n \varphi(r) dr \quad (17)$$

is the  $n$ th moment of PSD.

The accuracy of calculations according to Eq. (14) is demonstrated in Fig. 1 for the gamma PSD  $\varphi(r) = Br^\mu \exp(-\mu r/r_0)$ , where  $B$  is the normalization constant (see Table 1),  $\mu=6$ , and  $r_0$  is the mode radius related to the effective radius  $r_{ef} \equiv M_{32}$  by the analytical equation  $r_{ef} = r_0(1+3/\mu)$ . The values  $M_{32}$  and  $M_{42}$  [see Eq. (16)] are given in Table 1 both for gamma and lognormal PSDs. The value of  $M_{62}$  shown in Table 1 appears in the asymptotic analysis of Eq. (14) as  $\theta \rightarrow 0$ . That is, it follows at small scattering angles that

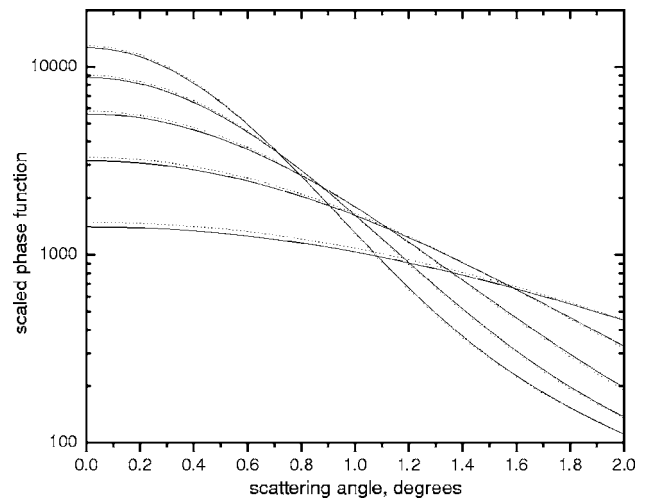


Fig. 1. Phase function of spherical polydispersions with effective radius of 4, 6, 8, 10, and 12  $\mu\text{m}$  [lower lines as  $\theta \rightarrow 0$  correspond to smaller particles (see Eq. (15) starting from  $a_{ef} = 4 \mu\text{m}$ ]. Results obtained using Mie theory are shown by solid curves and the approximation is given by dotted curves. Calculations have been performed for the gamma PSD with the half-width parameter  $\mu=6$  and  $\lambda=0.5 \mu\text{m}$ . The complex refractive index  $m=1.52-0.008i$  was used in exact numerical calculations.

**Table 1. Selected Ratios of Moments for Gamma and Lognormal PSDs**

Parameter	Gamma PSD	Lognormal PSD
	$Br^\mu \exp\left[-\mu \frac{r}{r_0}\right]$	$Br^{-1} \exp\left[-\frac{1}{2\sigma^2} \ln^2 \frac{r}{r_m}\right]$
$B$	$\frac{\mu^{\mu+1}}{r_0^{\mu+1} \Gamma(\mu+1)}$	$\frac{1}{\sigma\sqrt{2\pi}}$
$r_{ef} \equiv M_{32}$	$r_0 \left[1 + \frac{3}{\mu}\right]$	$r_m \exp\left[\frac{5}{2}\sigma^2\right]$
$M_{42}$	$\frac{\mu+4}{\mu+3} r_{ef}^2$	$r_{ef}^2 \exp\left[-\frac{1}{4}\sigma^2\right]$
$M_{64}$	$\frac{(\mu+5)(\mu+6)}{(\mu+3)^2} r_{ef}^2$	$r_{ef}^2 \exp\left[\frac{15}{4}\sigma^2\right]$

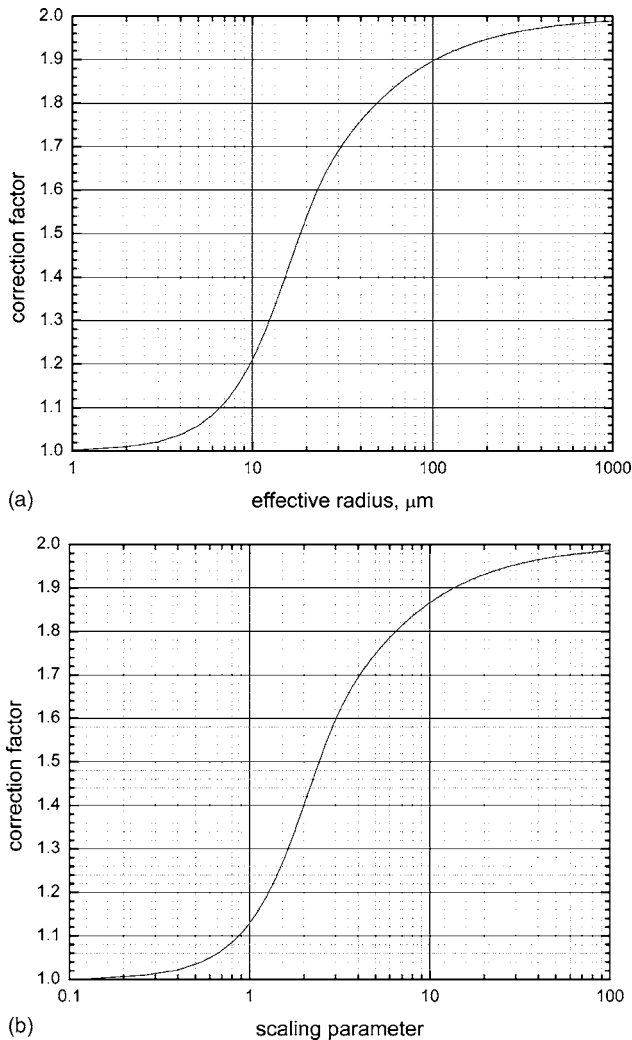


Fig. 2. Dependence of correction factor on (a) effective radius ( $\theta_0 = 0.6^\circ$ ) and (b) scaling parameter. The input for calculations is the same as for Fig. 1.

$$\hat{p}(\theta) = \frac{k^2 M_{42}}{2} \left( 1 - \frac{k^2 M_{64} \theta^2}{4} \right). \quad (18)$$

We conclude from the analysis of Fig. 1 that Eq. (14) can be used instead of tedious Mie calculations at  $\rho_{ef}$

$\equiv ka_{ef} \gg 1$  and small scattering angles. It follows from this figure that the accuracy of Eq. (14) increases with the radius at small scattering angles ( $\theta \rightarrow 0$ ) as one might expect. We also see that Eq. (14) works well for all angles relevant to the performance of Sun photometers with a narrow FOV. Therefore, we can use Eq. (14) to perform the integration as shown in Eq. (6). The solution is

$$f = \frac{1}{2} [1 - \langle J_0^2(k\theta_0 r) \rangle - \langle J_2^2(k\theta_0 r) \rangle], \quad (19)$$

where the meaning of angular brackets is explained above. Bessel functions  $J_0$  and  $J_2$  approach zero at large values of the argument  $z = k\theta_0 r$ . This means that it follows for very large values of  $z$  that  $f = 1/2$  and  $C = 2$  [see Eq. (9)].

By using Eqs. (8), (9), and (19) we obtain

$$\tau = \frac{\tau_0}{1 - \frac{1}{2} [1 - \langle J_0^2(k\theta_0 a) \rangle - \langle J_2^2(k\theta_0 a) \rangle]}, \quad (20)$$

and, therefore, finally

$$C = \frac{2}{1 + \langle J_0^2(k\theta_0 a) \rangle + \langle J_2^2(k\theta_0 a) \rangle}. \quad (21)$$

This gives an analytical solution for the CF depending on both FOV and PSD in the case of large scatterers. The results of calculations using Eq. (21) are shown in Fig. 2 as functions of both the effective radius  $a_{ef}$  [Fig. 2(a)] and the scaling parameter  $z_{ef} = ka_{ef}\theta_0$  [Fig. 2(b)]. Data shown in Fig. 2(a) have been obtained using  $\theta_0 = 0.6^\circ$ , which coincides with the half-FOV angle of widely used and commercially available AERONET Cimel Sun-sky photometers.<sup>6</sup>

One concludes from this figure that  $C$  is smaller than 1.2 for most aerosol particles ( $a_{ef} < 10 \mu\text{m}$ ). However, for the case of desert dust close to its origin the values of  $C$  can be much larger due to generally larger sizes of suspended dust grains. Yet another problem is due to thin cirrus clouds. Particles in these clouds are of the order of  $100\text{--}1000 \mu\text{m}$  and the correction factor is close to 2. This means that the apparent optical thickness as detected at the ground for the case of a thin cirrus cloud must be multiplied by 2. A similar result has been established in other work<sup>2,4,5</sup> for various values of  $\theta_0$ . The physical analysis of the problem shows that the value of  $\theta_0$  does not affect the condition  $C = 2$  as far as the whole diffraction peak is contained inside the FOV of the instrument. This is the case for practically all Sun photometers. In particular, we estimate that  $\theta_0$  must be larger than  $0.2^\circ$  to hold the whole diffraction peak in the FOV of the instrument for the case of monodispersed spherical particles with  $r = 100 \mu\text{m}$ .

### 3. ACCOUNTING FOR MULTIPLE LIGHT SCATTERING

Aerosol media with large particles can also have a large optical thickness. Then the single scattering approximation considered in Section 2 is not valid. Let us derive the CF for the case of a homogeneous plane parallel layer tak-

ing into account multiple light scattering. For this the integrodifferential radiative transfer equation must be solved. This equation has the following form for the case of the nadir illumination of a scattering layer<sup>9</sup>:

$$\mu \frac{dI(\mu, \tau)}{d\tau} = -I(\mu, \tau) + \frac{\omega_0}{2} \int_{-1}^1 I(\tau, \eta) \bar{p}(\eta, \mu) d\eta, \quad (22)$$

where  $I$  is the total light intensity including the diffused and direct components, and

$$\bar{p}(\mu, \eta) = \sum_{j=0}^{\infty} h_j P_j(\mu) P_j(\eta) \quad (23)$$

is the azimuthally averaged phase function,  $P_j(\mu)$  is the Legendre polynomial, and  $h_j$  are coefficients in the expansion of the phase function as shown by

$$p(\theta) = \sum_{j=0}^{\infty} h_j P_j(\cos \theta). \quad (24)$$

The value of  $\mu$  in Eq. (22) is the cosine of the observation angle, which is assumed to be close to 1 in this work because we consider directions  $\mu \approx \mu_0 = 1$  important for Sun photometry. Then it follows from Eq. (22) that

$$\frac{dI(\mu, \tau)}{d\tau} = -I(\mu, \tau) + \frac{\omega_0}{2} \int_{-1}^1 I(\tau, \eta) \bar{p}(\eta, \mu) d\eta. \quad (25)$$

This equation can be solved using the substitution<sup>10</sup>

$$I(\mu, \tau) = \sum_{j=0}^{\infty} \nu_j(\tau) P_j(\mu) \quad (26)$$

and also the expansion given by Eq. (23). One then easily derives

$$\frac{d\nu_j}{d\tau} = -\nu_j + \frac{\omega_0 h_j}{2j+1} \nu_j, \quad (27)$$

where we used the normalization condition

$$\int_{-1}^1 P_i(\eta) P_j(\eta) d\eta = \frac{2}{2j+1} \delta_{ij}. \quad (28)$$

Here  $\delta_{ij}$  is equal to one at  $i=j$  and zero otherwise. It follows after integration of Eq. (27) that

$$\nu_j = A_j \exp(-c_j \tau), \quad (29)$$

where

$$c_j = 1 - \frac{\omega_0 h_j}{2j+1} \quad (30)$$

and  $A_j$  are constants that can be determined from boundary conditions. In particular, we will assume that

$$I(\mu, 0) = E_0 \delta(1 - \mu). \quad (31)$$

Then using the expansion

$$\delta(1 - \mu) = \frac{1}{4\pi} \sum_{j=0}^{\infty} (2j+1) P_j(\mu), \quad (32)$$

we derive

$$A_j = \frac{E_0}{4\pi} (2j+1). \quad (33)$$

Therefore, it follows, finally, for the total transmitted light intensity that

$$I(\mu) = \frac{E_0}{4\pi} \sum_{j=0}^{\infty} (2j+1) \exp(-c_j \tau) P_j(\mu). \quad (34)$$

One obtains from Eq. (34) for the diffused light intensity

$$I_{dif}(\mu) = \frac{E_0}{4\pi} \sum_{j=0}^{\infty} (2j+1) [\exp(-c_j \tau) - \exp(-\tau)] P_j(\mu), \quad (35)$$

where we have subtracted the direct beam component [see Eqs. (3), (31), and (32)],

$$I_{dir}(\mu) = \frac{E_0 \exp(-\tau)}{4\pi} \sum_{j=0}^{\infty} (2j+1) P_j(\mu). \quad (36)$$

Equation (35) coincides with Eq. (4) as  $\tau \rightarrow 0$ , as one might expect. That is, it follows in this case that

$$I_{dif}(\mu) = \frac{E_0 \tau}{4\pi} \sum_{j=0}^{\infty} (2j+1) (1 - c_j) P_j(\mu), \quad (37)$$

or, after using Eqs. (24) and (30),

$$I_{dif}(\mu) = \frac{\omega_0 E_0 p(\theta) \tau}{4\pi}, \quad (38)$$

which is equivalent to Eq. (4) as  $\tau \rightarrow 0$ ,  $\mu_0 \rightarrow 1$ . Therefore, we conclude that Eq. (35) has a correct limit at small optical thicknesses.

Now we take into account that we are interested in the region of very small observation angles  $\vartheta = \arccos(\mu) \approx \theta$ . Then the following asymptotical relationship holds:  $P_j(\cos \theta) = J_0(\alpha_j \theta)$ , where  $\alpha_j = j + 1/2$  and  $J_0$  is the Bessel function. Therefore, Eq. (35) can be rewritten as

$$I_{dif}(\theta) = \frac{E_0 \exp(-\tau)}{2\pi} \sum_{j=0}^{\infty} \alpha_j [\exp(\kappa_j \tau) - 1] J_0(\alpha_j \theta), \quad (39)$$

where

$$\kappa_j = \frac{\omega_0 h_j}{2j+1}. \quad (40)$$

Let us introduce the transmission function<sup>10</sup>

$$T = \frac{\pi I_{dif}}{\mu_0 E_0}. \quad (41)$$

Then it follows that

$$T = \frac{\exp(-\tau)}{2} \sum_{j=0}^{\infty} \alpha_j [\exp(\kappa_j \tau) - 1] J_0(\alpha_j \theta). \quad (42)$$

This function does not depend on the azimuth due to the symmetry of the problem. The comparison of calculations of the transmission function according to Eq. (42) with exact radiative transfer numerical simulations using the

vector code SCIAPOL<sup>11</sup> is shown in Fig. 3 at  $\theta=1^\circ$ . The code is freely distributed at [www.iup.physik.uni-bremen.de/~alexk](http://www.iup.physik.uni-bremen.de/~alexk). It follows that both methods give the same results for all practical purposes related to Sun photometry. Therefore, Eq. (39) can be used instead of the tedious numerical solution of the exact radiative transfer equation. It follows from Fig. 4 that the approximate theory described here holds up to  $\tau=25$  for the case considered above.

Summing up, we conclude that Eq. (39) can be used for the analysis of scattered light in the FOV of Sun photometers at any  $\tau$  of practical interest. However, the angular range of applicability is generally reduced with optical thickness. This is studied in Figs. 5–7. It follows that Eq. (42) can be used at  $\theta < 10^\circ$  and any  $\tau$  relevant to observations of the direct light with a high accuracy. As a matter of fact the numerical solutions of the radiative transfer equation can benefit from the use of Eq. (42), because this formula considerably increases the speed of calculation without any loss of accuracy at small angles.

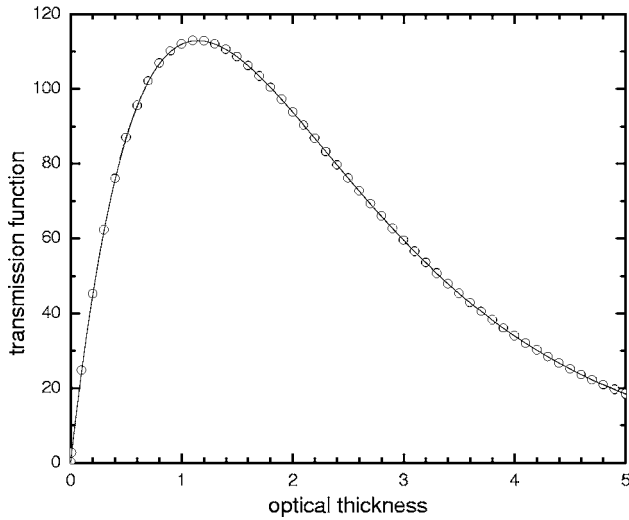


Fig. 3. Dependence of transmission function at  $\theta=1^\circ$  on optical thickness according to the approximation (solid curve) and exact calculations (open circles) at  $a_{ef}=4 \mu\text{m}$ . Other input parameters are as for Fig. 1.

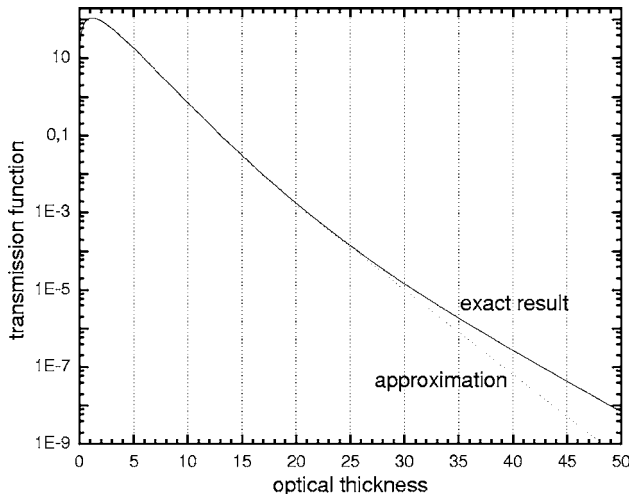


Fig. 4. Same as Fig. 3 except in a broader range of  $\tau$ .

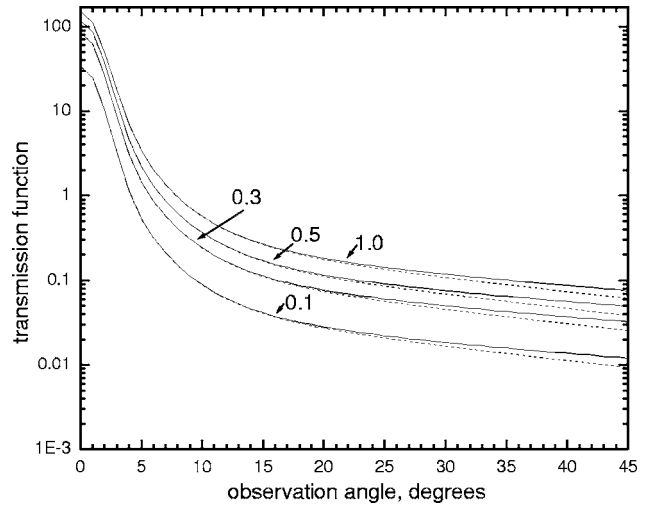


Fig. 5. Comparison of the exact theory (solid curves) and approximation (dotted curves) for different values of optical thickness (0.1, 0.3, 0.5, 1.0) and  $a_{ef}=4 \mu\text{m}$ . Other input parameters are as for Fig. 1.

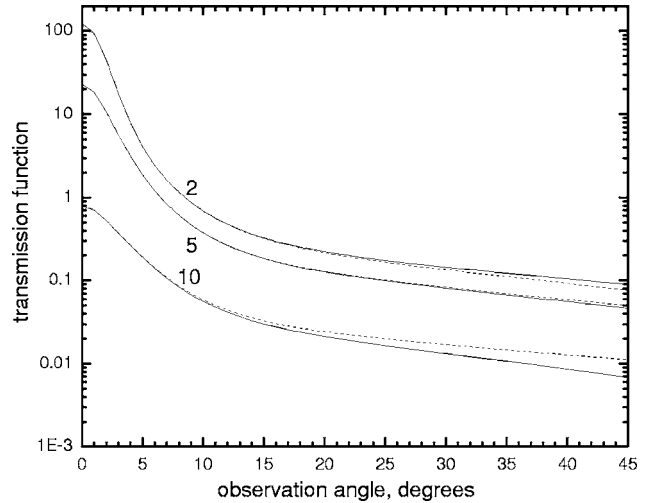


Fig. 6. Same as Fig. 5 except at  $\tau=2, 5, 10$ .

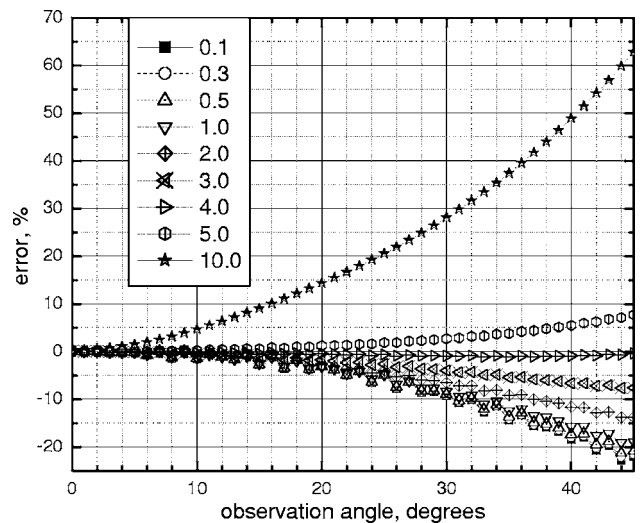


Fig. 7. Error of the approximation at different values of  $\tau$  shown in the legend and  $a_{ef}=4 \mu\text{m}$ .



We have proved that Eq. (39) is very accurate as far as its applications to Sun photometry are of concern. Therefore, it can be used to find the diffused light power  $F_{dif}$  in the FOV of the instrument [see Eq. (2)]. It follows after the azimuthal integration that

$$F_{dif} = \Sigma E_0 \exp(-\tau) \sum_{j=0}^{\infty} \alpha_j [\exp(\kappa_j \tau) - 1] D_j(\theta_0), \quad (43)$$

where

$$D_j(\theta_0) = \int_0^{\theta_0} J_0(\alpha_j \theta) \sin \theta d\theta. \quad (44)$$

This integral can be evaluated analytically taking into account that  $\theta_0 \ll 1$ . Then it follows that

$$D_j(\theta_0) = \frac{\theta_0 J_1(\alpha_j \theta_0)}{\alpha_j}, \quad (45)$$

where we used the integral

$$\int J_0(s) s ds = s J_1(s), \quad (46)$$

and the fact that  $\sin \theta \approx \theta$  at small angles.

Finally, one obtains from Eqs. (43) and (45) that

$$F_{dif} = \Sigma E_0 \theta_0 \psi(\tau) \exp(-\tau), \quad (47)$$

where

$$\psi(\tau) = \sum_{j=0}^{\infty} [\exp(\kappa_j \tau) - 1] J_1(\alpha_j \theta_0). \quad (48)$$

Therefore, the problem of the evaluation of the diffused light power as observed by a Sun photometer is reduced to the calculation of simple series. It follows from Eq. (47) that  $F_{dif} = 0$  at  $\theta_0 = 0$ , the result one can expect from the general consideration of the problem at hand. Clearly, the total power follows as

$$F = \Sigma E_0 [1 + \theta_0 \psi(\tau)] \exp(-\tau), \quad (49)$$

where we added the direct light contribution. Equation (49) can be also written in the form

$$F = \Sigma E_0 \exp(-\tau_0), \quad (50)$$

where

$$\tau_0 = \tau [1 - \gamma(\tau)], \quad (51)$$

and

$$\gamma(\tau) = \frac{1}{\tau} \ln[1 + \theta_0 \psi(\tau)]. \quad (52)$$

Finally, we obtain the following expression for the correction factor  $C \equiv \tau/\tau_0$  [see Eq. (51)]:

$$C = \frac{1}{1 - \gamma(\tau)}. \quad (53)$$

This factor depends not only on the size of particles as in the case of the single scattering approximation [see Eq. (21)] but also on the value of  $\tau$ . Also Eq. (51) is more general as compared with Eq. (21) because instead of ap-

proximation (14), coefficients  $h_j$  obtained from the Mie theory are used.

It follows from Eq. (48) at  $\tau \ll 1$  that

$$\psi(\tau) = \tau \sum_{j=0}^{\infty} \kappa_j J_1(\alpha_j \theta_0), \quad (54)$$

and therefore

$$\gamma = \theta_0 \sum_{j=0}^{\infty} \kappa_j J_1(\alpha_j \theta_0), \quad (55)$$

where we used an approximate equality  $\ln(1+x) \approx x$  valid at small  $x$ . Equation (55) can be rewritten in the following form [see Eq. (40)]:

$$\gamma = \frac{\omega_0}{2} \theta_0 \sum_{j=0}^{\infty} \frac{h_j J_1(\alpha_j \theta_0)}{\alpha_j}, \quad (56)$$

or taking into account Eqs. (44), (45), (24), and (6), it follows that  $\gamma \rightarrow f$  as  $\tau \rightarrow 0$ , where we also substituted the Bessel function by the Legendre polynomial, which is a valid operation at small scattering angles. Therefore, Eq. (9) is a particular case of Eq. (53) valid at small optical thicknesses. This confirms our calculations.

The dependence of  $C$  on  $\tau$  [see Eqs. (53), (52), and (48)] is shown in Fig. 8. Coefficients  $h_j$  (see Fig. 9) and also  $\omega_0$  have been calculated for the gamma PSD at  $\lambda = 0.5 \mu\text{m}$ , the dust refractive index<sup>9</sup>  $m = 1.52 - 0.008i$ ,  $\mu = 6$ , and several values of  $a_{ef}$  using the Mie theory. The computed values of the single scattering albedo  $\omega_0$  varied from  $0.55(a_{ef} = 30 \mu\text{m})$  to  $0.75(a_{ef} = 2 \mu\text{m})$ .

We conclude from Fig. 8 that correction factors are not significantly affected by the value of  $\tau$ . This is similar to the findings of others<sup>4,6</sup> and means that simple Eq. (21) can be used for the estimation of correction factors in the case of aerosol media with large scatterers at arbitrary values of  $\tau$  relevant to observation of attenuation of the direct light.

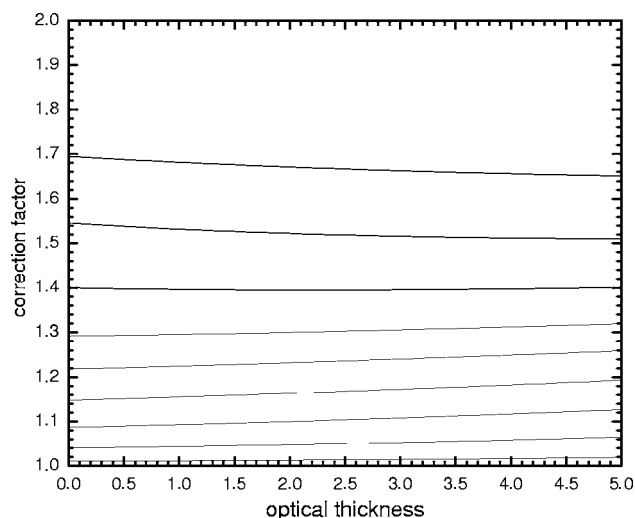


Fig. 8. Dependence of correction factor on optical thickness at  $\theta_0 = 0.6^\circ$  and  $a_{ef} = 2, 4, 6, 8, 10, 12, 15, 20$ , and  $30 \mu\text{m}$ . Lower curves correspond to smaller sizes starting from  $a_{ef} = 2 \mu\text{m}$ . (The coefficients  $\kappa_j$  have been calculated using the Mie theory for the same conditions as for Fig. 1; they are shown in Fig. 9.)

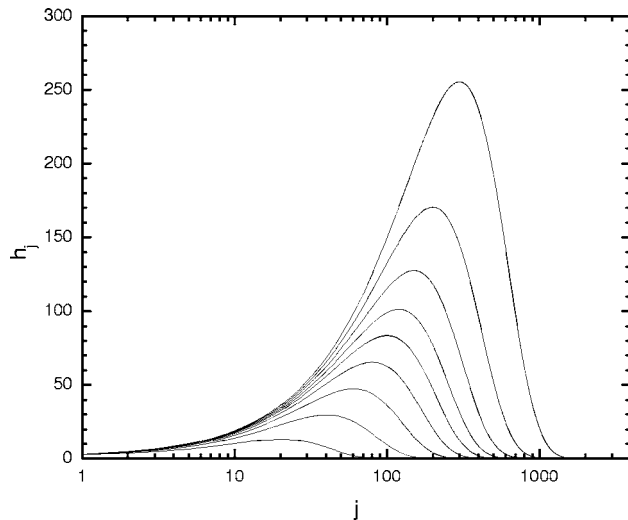


Fig. 9. Coefficients  $h_j$  for the cases shown in Fig. 8. Lower curves correspond to smaller sizes starting from  $a_{\text{eff}} = 2 \mu\text{m}$ .

Results as shown in Fig. 8 are difficult to obtain from numerical calculations using the exact radiative transfer equation because it involves the study of light intensity at small angles, where many hundreds of Legendre polynomials are needed to represent the small-angle peak in a correct way (see Fig. 9). The use of simple series given by Eq. (48) allows us to perform such calculations accurately and in a short time for an arbitrary number of Legendre polynomials relevant to aerosol and cloud optics problems. A shortcoming is that only the normal illumination conditions can be analyzed using Eqs. (42) and (48). The consideration of the case of a slant illumination relevant for most cases requires numerical calculations using the exact radiative transfer equation.<sup>4,10</sup> However, the low sensitivity of  $C$  to  $\tau$  shown in Fig. 8 also means that  $C$  is weakly influenced by the solar zenith angle. Therefore, Eq. (21) can also be used for values of  $\mu_0$  different from 1 also at comparatively large  $\tau$ . The reason for this is quite clear: The contribution of scattered light to the FOV of photometers having small values of  $\theta_0$  is due mostly to single scattering and not to multiple light scattering.

#### 4. CONCLUSIONS

We derived the approximate equations for the scattered light correction factors for Sun photometers in the special case when the diffused light detected by an instrument is mostly due to light scattering by large airborne particles. The explicit dependence of correction factors on the size of particles and also on the optical thickness of the medium is given.

The sizes of particles are often not known in advance. Therefore, the results presented here can be used only for the estimation of corresponding corrections for different sizes and not for the determination of  $\tau$  except for the cases when the particles are very large (say,  $100 \mu\text{m}$  for the visible light) and  $C=2$ .

If the particles are large and the PSD is not precisely known, then the atmospheric optical thickness cannot be found from measurements of a Sun photometer directed

just to the Sun.<sup>5</sup> Diffuse sky brightness at several wavelengths must also be measured in addition to the spectra of transmitted light. The measured data can be used in the retrieval procedure involving the radiative transfer equation solution.<sup>12,13</sup> This makes retrieval of  $\tau$  much more complicated as compared with interpretation of just transmitted light for the cases of comparatively clear skies in the absence of large scatterers.

The results presented in this work are very general. In particular, they can be applied also for particles having refractive indices other than those studied in this work. This is because scattering of light at small angles is not influenced by the refractive index if conditions specified in the paper are satisfied.

Equation (42) can be used to study the influence of multiple light scattering on the performance of modern optical particle sizing instruments.<sup>9</sup> Then the geometry of the experiment ( $\vartheta \approx \vartheta_0 = 0$ ) completely coincides with the case studied in this work.

The author's e-mail address is alexk@iup.physik.uni-bremen.de.

#### REFERENCES

1. W. von Hoyningen-Huene, "Untersuchung von Optischen Eigenschaften einer Aerosolhaltigen Atmosphäre zur Ableitung von Aerosolparametern und ihrer Bedeutung für Kurzwelligigen Strahlungstransfer," Habilitation thesis (Leipzig University, 1975).
2. M. Shiobara and S. Asano, "Estimation of cirrus optical thickness from Sun photometer measurements," *J. Appl. Meteorol.* **33**, 672–681 (1988).
3. R. G. Timanovskaya, "Optical parameters of cirrus clouds obtained using ship observations of direct solar light," *Izv. Acad. Sci. USSR Atmos. Oceanic Phys.* **30**, 258–262 (1994).
4. E. P. Zege, I. L. Katsev, I. N. Polonsky, and A. S. Prikhach, "Effect of scattered light on accuracy of measurements of thin cloud optical thickness by a Sun photometer," *Izv. Acad. Sci. USSR Atmos. Oceanic Phys.* **30**, 308–316 (1994).
5. P. P. Anikin, "Optical thickness of semitransparent clouds and evaluation of cloud particle size," *Izv. Acad. Sci. USSR Atmos. Oceanic Phys.* **30**, 231–236 (1994).
6. P. B. Russel, J. M. Livingston, O. Dubovik, S. A. Ramirez, J. Wang, J. Redemann, B. Schmid, M. Box, and B. N. Holben, "Sunlight transmission through desert dust and marine aerosols: diffuse light corrections to Sun photometry and pyrrometry," *J. Geophys. Res.* **109**, D08207 doi: 10.1029/2003jd004292 (2004).
7. A. Ishimaru, *Wave Propagation and Scattering in Random Media* (Oxford U. Press, 1997).
8. H. C. van de Hulst, *Light Scattering by Small Particles* (Dover, 1981).
9. A. A. Kokhanovsky, *Light Scattering Media Optics* (Springer-Praxis, 2004).
10. E. P. Zege, A. P. Ivanov, and I. L. Katsev, *Image Transfer through a Scattering Medium* (Springer, 1991).
11. V. V. Rozanov and A. A. Kokhanovsky, "The solution of the vector radiative transfer equation using the discrete ordinates technique: selected applications," *Atmos. Res.* **79**, 241–265 (2006).
12. W. von Hoyningen-Huene and P. Posse, "Nonsphericity of aerosol particles and their contribution to radiative forcing," *J. Quant. Spectrosc. Radiat. Transf.* **57**, 651–688 (1997).
13. O. Dubovik and M. D. King, "A flexible inversion algorithm for retrieval of aerosol optical properties from Sun and sky radiance measurements," *J. Geophys. Res.* **105**, 20673–20696 (2000).